Published in final edited form as:
J Med Chem. 2013 March 14; 56(5): 2139–2149. doi:10.1021/jm400050y.

Opioid Peptidomimetics: Leads for the Design of Bioavailable Mixed Efficacy Mu Opioid Receptor (MOR) Agonist/Delta Opioid Receptor (DOR) Antagonist Ligands

Henry I. Mosberg[1,2,*], **Larisa Yeomans**[1], **Aubrie A. Harland**[2], **Aaron M. Bender**[2], **Katarzyna Sobczyk-Kojiro**[1], **Jessica P. Anand**[2], **Mary J. Clark**[3], **Emily M. Jutkiewicz**[3], and **John R. Traynor**[3]

[1]Department of Medicinal Chemistry, College of Pharmacy, University of Michigan, Ann Arbor, MI 48109

[2]Interdepartmental Program in Medicinal Chemistry, University of Michigan, Ann Arbor, MI 48109

[3]Department of Pharmacology, Medical School, University of Michigan, Ann Arbor, MI 48109

Abstract

We have previously described opioid peptidomimetic, **1**, employing a tetrahydroquinoline scaffold and modeled on a series of cyclic tetrapeptide opioid agonists. We have recently described modifications to these peptides that confer a mu opioid receptor (MOR) agonist, delta opioid receptor (DOR) antagonist profile, which has been shown to reduce the development of tolerance to the analgesic actions of MOR agonists. Several such bifunctional ligands have been reported, but none has been demonstrated to cross the blood brain barrier. Here we describe the transfer of structural features that evoked MOR agonist/DOR antagonist behavior in the cyclic peptides to the tetrahydroquinoline scaffold and show that the resulting peptidomimetics maintain the desired pharmacological profile. Further, the *4R* diastereomer of **1** was fully efficacious and approximately equipotent to morphine in the mouse warm water tail withdrawal assay following intraperitoneal administration and thus a promising lead for the development of opioid analgesics with reduced tolerance.

Introduction

The recognition that the simultaneous modulation of multiple targets may generate a more desirable drug profile has challenged the long prevailing, intuitive bias toward selectively targeted drugs as the optimal approach for the discovery and development of new therapeutics (for recent reviews see [1–3]). This concept is exemplified in the field of opioid analgesics by the observation that co-administration of a mu opioid receptor (MOR) agonist with a delta opioid receptor (DOR) antagonist retains MOR-mediated analgesia, but displays reduced development of tolerance and dependence[4–6], features that limit the clinical use of opioid analgesics.

For pharmacokinetic simplicity it is preferable to incorporate all desired activities into a single compound, and the development of bifunctional opioid ligands has thus become a topic of increasing interest. For many years, our focus had been on receptor selective opioids. While structure-activity efforts toward this aim were quite successful, a number of 'failures' – including ligands that displayed high affinity for both MOR and DOR – resulted and were not pursued further. The subsequent accumulation of convincing evidence for the

*Corresponding Author Information: Henry I. Mosberg; him@umich.edu; phone: (734)764-8117.

value of MOR agonist/DOR antagonist ligands encouraged us to reinvestigate our earlier non-selective peptides. This reinvestigation led to the development of a cyclic tetrapeptide Tyr-c(SEtS)[D-Cys-Aic-D-Pen]OH (**KSK103**)[7], where Aic is 2-aminoindane, 2-carboxylic acid; Pen is penicillamine; and c(SEtS) designates cyclization through the D-Cys and D-Pen side chain sulfurs as an ethylene dithioether. This peptide exhibits high affinity for MOR and DOR (and low affinity for the kappa opioid receptor, KOR) and is a MOR agonist/DOR antagonist[7]. Follow-up studies[8] revealed that steric bulk and conformational constraint of the Aic or similar substitutions were key factors for achieving *in vitro* MOR agonism/DOR antagonism in this series.

Other peptide[9], peptide-like[10, 11], and non-peptide[12] structures have been reported that display MOR agonist/DOR antagonist profiles, however none of these has demonstrated centrally mediated *in vivo* activity after peripheral administration. This poor bioavailability is typical of peptides and, while several approaches have been demonstrated to improve peptide penetration of biological membranes[13–15], the alternative strategy of incorporating the key pharmacophore elements of a peptide with desired pharmacological properties into a more drug-like scaffold provides a more direct strategy toward improved bioavailability. The main hurdle that must be cleared in the latter approach is assuring that the resulting peptidomimetic does indeed demonstrate the desired pharmacological profile.

We have previously described the peptidomimetic diastereomeric pair, **1**, designed to incorporate the key opioid pharmacophore elements of the parent tetrapeptide Tyr-c(SS)[D-Cys-Phe-D-Pen]OH, **2** (**JOM-13** [16], Figure 1) and related cyclic tetrapeptides, namely a tyramine moiety and a second aromatic group, attached to a tetrahydroquinoline (THQ) scaffold[16]. This design strategy proved to be successful, as the higher affinity diastereomer of **1** displayed high binding affinity to MOR, DOR and KOR[14]. Our observation that Aic and other replacements for Phe in cyclic peptides related to **2** confer a MOR agonist/DOR antagonist profile, suggested that **1** might be a promising starting point for the development of related peptidomimetics with similar profiles, but with improved bioavailability compared to the peptides. Here we establish that the higher affinity diastereomer of **1** is the *4R* diastereomer (**1**(*4R*)) and demonstrate that a.) **1**(*4R*) displays a promising *in vitro* profile with high MOR efficacy and low DOR efficacy; b.) **1**(*4R*) is approximately equipotent to morphine in the antinociceptive mouse warm water tail withdrawal assay after intraperitoneal administration, thus showing great promise as a lead for the development of a bioavailable MOR agonist/DOR antagonist; and c.) that modifications that confer high MOR efficacy/low DOR efficacy in our cyclic peptide series, retain this effect when used as replacements for the benzyl pendant on the THQ scaffold of **1**.

Results

Synthesis of 1

Our original synthesis of **1** yielded the *4R* and *4S* diastereomeric pair, which were easily separated by RP-HPLC and pharmacologically evaluated individually, with the observation that the diastereomer that elutes earlier on HPLC displays 5–10 fold higher binding affinity at MOR, DOR, and KOR than the later eluting diastereomer. In order to confirm the stereochemistry of **1**, we undertook an asymmetric synthesis (Scheme 1). Briefly, ketone intermediate **3** was Boc protected to give **4**, which was reduced with the (*S*)-methyl-CBS catalyst[17] to give chiral, *4R* alcohol **5** in 80% ee, similar to previous reports for analogous scaffolds[17, 18]. The secondary chiral alcohol was then converted to an amine, with complete inversion of stereochemistry *via* a Mitsunobu reaction[19], yielding chiral, *4S* amine **7** to which di-Boc protected 2,6-dimethyl-L-tyrosine (Boc-Dmt) was coupled. After deprotection of this unequivocal *4S* diastereomer, HPLC revealed a 9:1 ratio of late eluting to early

eluting diastereomer of **1**, confirming that the late eluting diastereomer is *4S* and the (higher affinity) early eluting diastereomer is *4R*, depicted in Figure 1.

Opioid receptor binding and efficacy

Binding affinities (K_i) (obtained by competitive displacement of radiolabeled [^{3}H] diprenorphine in C6 cells stably expressing MOR or DOR or CHO cells stably expressing KOR, as previously described[20, 21]) for both diastereomers of **1** and efficacy (assessed by agonist-stimulated [^{35}S] GTPγS binding in the same cells[22]) at MOR, DOR, and KOR of the higher affinity *4R* diastereomer are shown in Tables 1 and 2, respectively. As shown in Table 1 the now confirmed *4R* diastereomer of **1** displays very high MOR affinity, and is approximately 40- and 300-fold selective for MOR *vs.* DOR or KOR, respectively. The *4S* diastereomer shows significantly lower affinity, especially at MOR. As seen in Table 2, the *4R* diastereomer of **1** shows high MOR potency and efficacy in the stimulation of GTPγS binding assay. Consistent with the binding data, the potency of **1**(*4R*) is much lower at DOR and KOR. Of special interest is the observation that **1**(*4R*) is a partial agonist at DOR and KOR, displaying only 16% and 22% maximal stimulation compared to the standards DPDPE and U69,593, respectively, suggesting a very promising starting point for the development of MOR agonist/DOR antagonist analogs.

Since, as described above, other MOR agonist/DOR antagonist ligands have been reported, the promise of THQ scaffold peptidomimetics like **1** is dependent on the ability of compounds in such a series to display centrally mediated effects after peripheral administration, a property not yet demonstrated for other MOR agonist/DOR antagonist ligands. Thus we examined the antinociceptive activity of the lead compound **1**(*4R*) in the mouse warm water tail withdrawal (WWTW) antinociception assay[23] following intraperitoneal (*ip*) administration.

The dose-response curve for **1**(*4R*) in the WWTW assay is presented in Figure 2 which shows that **1**(*4R*) produces a dose dependent increase in tail withdrawal latency (up to the 20s cutoff) with an ED_{50} ~3mg/kg (~6 μmol/kg). Figure 2 further shows that this antinociceptive effect is opioid receptor mediated, since the opioid antagonist naltrexone at 1mg/kg *ip*, produces a rightward shift in the dose/response curve of **1**(*4R*). The time course of the antinociceptive activity of **1**(*4R*) in the WWTW assay, along with that for morphine, is shown in Figure 3. As seen there, **1**(*4R*) displays a rapid onset of effect and maximal antinociception is maintained for approximately 60 minutes, followed by a slow decline. The duration of action of **1**(*4R*) is somewhat shorter than that of morphine.

Encouraged by the antinociceptive activity and bioavailability of **1**(*4R*), we prepared a small series of analogs in which the benzyl side chain of **1** was replaced by bulkier or more constrained aromatic moieties. These replacements were based on results we had obtained in the tetrapeptide and pentapeptide series developed from **2**. Using computational models of active and inactive states of MOR and DOR[7, 8] we predicted and confirmed that replacing the Phe^3 residue in these tetra- or pentapeptides with a bulkier or more constrained aromatic residue would maintain MOR efficacy, but reduce DOR efficacy. In particular, 1-naphthylalanine (1-Nal), 2-naphthylalanine (2-Nal), and 2-aminoindane, 2-carboxylic acid (Aic), substitution for Phe all resulted in analogs that displayed MOR agonist/DOR antagonist behavior and maintained high affinity binding to both receptors[7, 8, 24]. Since peptidomimetic **1** was designed from 2 (Figure 1), we examined the effect of transferring the corresponding modifications to the THQ scaffold of **1** in place of the benzyl moiety (Figure 4), anticipating that, as in the peptide series, MOR agonist/DOR antagonist profiles would be observed.

Synthesis of peptidomimetic analogs of 1

Compounds **8a–b** were prepared by P_2O_5-catalyzed Friedel-Crafts acylation of benzene or naphthalene with the corresponding *p*-nitro carboxylic acid (Scheme 2)[25]. **8b** was synthesized as a mixture of the 1-naphthalene and 2-naphthalene products in a 1:4 ratio. **8c** was prepared by Suzuki coupling[26] between 2-naphthalene boronic acid *p*-nitro benzyl bromide, and **8d** was prepared by an aldol condensation between 1-indanone and *p*-nitro benzoic acid. The resulting nitro compounds were subjected to hydrogenation to afford amines **9a–d**, which were then acylated with 3-bromopropionyl chloride to afford **10a–d**. Cyclization with NaO*t*Bu formed the 4-membered lactams (**11a–d**), which were then rearranged under Fries conditions to give dihydroquinolinones **12a–d**[27]. Oxime formation (**13a–d**) and subsequent hydrogenation gave racemic primary amines **14a–d**, which could then be coupled to Boc-Dmt under standard peptide coupling conditions (Scheme 3).

The synthetic protocol described in Schemes 2 and 3 yields racemic mixtures of *4R* and *4S* scaffolds which are then used to generate the diastereomeric pairs of final peptidomimetics **15a** and **15a′; 15c** and **15c′**; and **15d** and **15d′**. The diastereomer of **15b** was observed but an insufficient amount for testing was isolated. In each pair, the 'unprimed' number (**15a–15d**) represents the diastereomer that elutes earlier in RP-HPLC, which in all cases is also the higher affinity diastereomer, as discussed below.

As was observed in our original report of **1**[16], the earlier eluting diastereomer of each tested pair displays 1–2 orders of magnitude higher MOR and DOR affinity compared with the later eluting diastereomer. Since the structural modifications within the series are rather minor and confined to the pendant moiety on the THQ scaffold, it is very likely that the higher affinity diastereomer in each of the new analogs is, as was observed for **1**, the 4*R* diastereomer. This would, of course, need to be confirmed for any analog chosen for extensive *in vivo* testing.

As seen in Table 1, all peptidomimetics bind with highest affinity at MOR (by a factor of 8 to 130) and, except for the diastereomeric pair **15d** and **15d′;**, all slightly prefer DOR over KOR. Efficacy data for the higher affinity diastereomers **1**(4*R*) and **15a–15d** are summarized in Table 2 as both EC_{50} and percent maximal stimulation compared to the standard agonists DAMGO, DPDPE, and U69,593 for MOR, DOR, and KOR, respectively. With the exception of **15a**, all the peptidomimetics tested display high efficacy at MOR and all are very potent, with EC_{50} values of ~ 1 nM. By contrast, none of these ligands significantly stimulate DOR, consistent with the desired MOR agonist/DOR antagonist profile, and only **15d** displays significant agonist properties at KOR. To confirm the desired MOR agonist/DOR antagonist profile, the ability of **15c**, a representative example from the series, to antagonize the stimulation of GTPγS binding evoked by the DOR agonist DPDPE was assessed. As expected, compound **15c** acted as a DOR antagonist, producing a rightward shift in the stimulation curve of DPDPE at DOR with K_e = 34.3 +/− 2.7 nM, in good agreement with the observed binding K_i of 10 nM for **15c** at DOR.

Discussion and Conclusions

Two results obtained with **1**(*4R*) are particularly noteworthy. First, the demonstration that this peptidomimetic modeled on a full agonist peptide, displays high MOR efficacy, but low DOR efficacy establishes it as strong lead for the development of MOR agonist/DOR antagonists using the THQ scaffold. The low DOR efficacy of **1**(*4R*) is consistent with our previously described models of interactions of opioid ligands with active and inactive states of the receptors[7, 8]. The binding pocket in the region of the Phe^3 sidechain of the tetrapeptide **2** and the benzyl substituent of the THQ scaffold of **1**(*4R*) (Figure 1C) includes Asn^{125}, Thr^{218}, and Lys^{303} in MOR and the corresponding, bulkier Lys^{108}, Met^{199}, and

Trp^{254} in DOR. The inactive state of both receptors can accommodate benzyl and even bulkier substituents, however these bulkier substituents clash with the larger residues of DOR in the more compact binding pocket found in the active state of the receptor, reducing efficacy at this receptor. As seen in the overlay of **1**(*4R*) with **2** in Figure 1C, the phenyl ring of **1**(*4R*) (red) extends farther (deeper into the DOR pocket) giving rise to its greater steric clash with the DOR active state, hence its reduced DOR efficacy compared to **2**.

The second critical observation for **1**(*4R*) is its promising bioavailability. As shown in Figures 2 and 3, 1(*4R*) displays antinociceptive activity in the mouse WWTW assay after *ip* administration and with similar potency as morphine. To date, no MOR agonist/DOR antagonist ligands have been reported that display central activity after peripheral administration, hence this represents a key result and promising lead.

The data in Tables 1 and 2 support the promise of this peptidomimetic series, as they demonstrate that features that confer DOR antagonism in our recently reported peptides[7, 8, 24] act similarly in the peptidomimetic series described here. For example, the 2-methylnaphthyl substituted **15c** reduces DOR efficacy compared to the 1-methylnaphthyl analog, **15b**. This mirrors observations made in the peptide series[8]. While all the peptidomimetics examined display low DOR efficacy, it appears that modifications with longer extended R (**15a**, **15c**, **15d** in Figure 1) are less compatible with the DOR active state. This is consistent with the observed low DOR efficacy of **1**(4*R*), compared with its DOR full agonist peptide counterpart **2** discussed above.

Compounds **15a–d**, like **1**(4*R*), are the higher affinity (and earlier eluting on HPLC) diastereomers of each pair and, given the structural similarity to **1**, most likely share the *4R* stereochemistry that was unequivocally determined for **1**(*4R*). Compounds **15a**–d all display fairly similar pharmacological profiles, with **15c** exhibiting the most promising combination of high MOR efficacy and potency, potent DOR antagonism, and somewhat reduced affinity (and no efficacy) at KOR. Compound **15d** displays a slightly different profile from the other members of the series in its considerably higher KOR affinity and smaller range of affinities across the three receptors. It also exhibits a potentially interesting MOR agonist/KOR partial agonist profile, a profile that may be useful for combating cocaine dependence[28–30]. Preliminary inspection of peptidomimetic docking to our receptor models suggests that the indanyl of **15d** can interact favorably with Val^{108} of transmembrane helix 2 (TM2) of the active conformation of KOR while the corresponding R substituent of the other peptidomimetics either adopt alternate low energy conformations or sterically clash with this region of the active state of KOR. Hence **15d** displays both higher KOR affinity and efficacy than the other analogs described here.

While the peptidomimetics described here show promise, their profiles require optimization before moving forward to *in vivo* tolerance studies. For example, the preferred MOR agonist/DOR antagonist ligand would display similar, high affinity for MOR and DOR, translating into potent, high efficacy MOR agonism and potent DOR antagonism, while interacting poorly with KOR. These preliminary results do, however, provide strong support for our structure-based design approach employing our ligand-receptor models and also lend confidence to our plans to further employ the THQ scaffold, which allows favorable interactions with MOR, DOR, and KOR, to ‘tune’ the pharmacological profile by incorporating modifications that exploit differences in nearby residues of MOR, DOR, and KOR in order to more closely equalize MOR and DOR binding affinity and reduce KOR affinity.

Finally, it should be mentioned that a MOR agonist/DOR antagonist profile is not unique in being associated with reduced development of tolerance and other MOR agonist side effects.

Several groups have described positive results with ligands that act as a MOR agonist/DOR agonist[31–34]. Included among these are ligands that are active after peripheral administration[31–33]. It is unclear whether DOR agonists and DOR antagonists exert their effects on MOR agonists in similar ways. For example, we showed that co-administration of a DOR agonist potentiates the potency and efficacy of morphine even in mice rendered tolerant to morphine[35]. Thus, it is possible that the reported reduction in MOR tolerance effected by DOR agonists reflects this potentiation of MOR agonist potency and/or efficacy.

Experimental Section

Chemistry

All reagents and solvents were obtained from commercial sources and used without additional purification. To prepare P_2O_5/Al_2O_3 (w/w 50%), Al_2O_3 was placed in an oven at 120° C for 24 h. After reaching room temperature in a desiccator, P_2O_5 was added in equal amounts, mixed and returned to the desiccator for later use. Suzuki couplings were performed on a Discover S-Class (CEM®) microwave in a closed vessel, with maximum power input 300W, and temperature set at 110°C for 10 minutes under the standard method from their Synergy software. Hydrogenations were performed on a Parr® hydrogenator apparatus from Parr Instrument Company, model 3916EA at the pressures specified using 10% Pd/C as the catalyst. Flash column chromatography was carried out using P60 silica gel (230–400 mesh). Purification of final compounds was performed using a Waters semipreparative HPLC with a Vydac Protein and Peptide C_{18} reverse phase column, using a linear gradient of 15% Solvent B (0.1% TFA in acetonitrile) in Solvent A (0.1% TFA in water) to 50% Solvent B in Solvent A at a rate of either 0.5% or 1% per minute and monitoring UV absorbance at 230 nm. Purity of synthesized compounds was determined on a Waters Alliance 2690 Analytical HPLC and a Vydac Protein and Peptide C_{18} reverse phase column, using a linear gradient of 0% Solvent B in Solvent A to 45%, 70%, or 90% Solvent B in Solvent A in 45 min, 70 min, or 90 min, respectively, and UV absorbance at 230 nm (gradient A). Purities of the final compounds used for testing were ≥ 95% pure as determined by HPLC. ^{1}H-NMR and ^{13}C-NMR data were obtained on either a 400 or 500 MHz Varian spectrometer using $CDCl_3$ or CD_3OD solvents. The identity of each compound was verified by mass spectrometry using an Agilent 6130 LC-MS mass spectrometer in positive mode.

General Procedure A for Compound 1

(*S*)-2-Amino-N-((*S*)-6-benzyl-1,2,3,4-tetrahydroquinolin-4-yl)-3-(4-hydroxy-2,6-dimethylphenyl)propanamide (1): The amine intermediate **7** (121 mg, 0.358 mmol) was dissolved in DMF (5 mL) followed by the addition of the coupling reagents PyBOP (186 mg, 0.358 mmol), HOBt-Cl (70.0 mg, 0.358 mmol) and DIEA (624 μL, 3.58 mmol). Boc-DMT (146 mg, 0.358 mmol) was dissolved in DMF (5 mL) and added to the reaction mixture, which was stirred for 18 h at room temperature. After concentration under reduced pressure the product was resuspended in EA (30 mL) and washed with a solution of 5% citric acid in H_2O (30 mL). The aqueous layer was then extracted with EA (10 mL), and the combined organic extracts were washed with brine (1 × 10 mL), dried with $MgSO_4$, filtered and concentrated under reduced pressure. The crude residue was dissolved in a 1:1 mixture of DCM and TFA (10 mL), and stirred for 3 h. The mixture was concentrated and purified by semipreparative HPLC to yield the title compound in a 9:1 ratio of diastereomers. HPLC (gradient A): retention time = 25.50 (early), 28.85 (late). EI-MS 452.2 $[M+Na]^+$ for both diastereomers.

Synthesis of Compounds 4–7

***Tert*-butyl 6-benzyl-4-oxo-3,4-dihydroquinoline-1(2*H*)-carboxylate (4):** Compound **3**[16] (2.57 g, 10.8 mmol) was dissolved in DCM (70 mL), followed by the addition of $(Boc)_2O$ (3.06 g, 14.1 mmol), DMAP (132 mg, 1.08 mmol) and DIEA (2.45 mL, 14.1 mmol). The mixture was stirred at reflux for 35 h, after which time it was quenched with 1M HCl (50 mL). The aqueous layer was extracted with DCM. The combined organic extracts were dried with $MgSO_4$, filtered and concentrated, and the residue was chromatographed on silica gel (1:2 EA/hex) to yield the title compound as a white solid (2.79 g, 77%). R_f (50% EA/hex): 0.71. ^{1}H-NMR (400 MHz, $CDCl_3$) δ 7.83 (d, *J* = 1.6, 1H), 7.69 (d, *J* = 1.6, 1H), 7.29 (dd, *J* = 8.6, 1.9, 1H), 7.26 – 7.19 (m, 2H), 7.18 – 7.10 (m, 3H), 4.08 (t, *J* = 6.2, 2H), 3.90 (s, 2H), 2.68 (t, *J* = 6.3, 2H), 1.53 (s, 9H); ^{13}C-NMR (101 MHz, $CDCl_3$) δ 194.23, 152.74, 142.37, 140.39, 134.61, 128.80, 128.54, 127.14, 126.26, 124.78, 123.81, 82.07, 44.26, 41.14, 38.97, 28.27.

(*R*)-*Tert*-butyl 6-benzyl-4-hydroxy-3,4-dihydroquinoline-1(2*H*)-carboxylate (5): Compound **4** (2.69 g, 7.97 mmol) was dissolved in THF (30 mL) and stirred at room temperature with 4Å-mol sieves (1.0 g) for 1 h. This solution was transferred to the (*S*)-(−)-2-methyl-CBS-oxazaborolidine catalyst via cannula and the reaction vessel was cooled to −20 °C. BH_3•Me_2S (3.99 mL, 7.97 mmol) was then added via syringe over a period of 10 min. The mixture was stirred at −20 °C for 6 h. After the addition of MeOH (7 mL) the reaction was allowed to reach room temperature. The mixture was partitioned between 1M HCl (10 mL) and Et_2O (30 mL). The aqueous layer was extracted with Et_2O (3 × 20 mL). The combined organic extracts were washed with brine (20 mL), dried with $MgSO_4$, filtered and concentrated, and the residue was chromatographed on silica gel (1:2 EA/hex) to yield the title compound as a colorless oil (2.19 g, 81%, 80% ee). R_f (50% EA/hex): 0.48. ^{1}H-NMR (400 MHz, $CDCl_3$) δ 7.72 (d, *J* = 8.5, 1H), 7.30 – 7.14 (m, 6H), 7.08 (dd, *J* = 8.16, 1.6, 1H), 4.53 (t, *J* = 4.8, 1H), 3.92 (s, 2H), 3.53 (ddd, *J* = 13.1, 9.5, 3.8, 1H), 3.40 (s, 1H), 1.98 – 1.90 (m, 1H), 1.89-1.79 (m, 1H), 1.56 (s, 9H); ^{13}C-NMR (101 MHz, $CDCl_3$) δ 153.73, 141.15, 135.71, 131.04, 128.92, 128.49, 128.25, 126.10, 123.57, 81.08, 65.47, 41.33, 40.74, 32.13, 28.43. Enantioselectivity determined by HPLC (Chiracel OD-RH column, 45% acetonitrile/water, 230 nm, 25 °C), t_{major} 21.3 min, t_{minor} 25.2 min.

(*S*)-*Tert*-butyl-6-benzyl-4-(1,3-dioxoisoindolin-2-yl)-3,4-dihydroquinoline-1(2*H*)-carboxylate (6): Compound **5** (2.12 g, 6.27 mmol) was dissolved in THF (25 mL) and added via syringe to a mixture of phthalimide (1.38 g, 9.40 mmol) and PPh_3 (2.47 g, 9.40 mmol). The reaction mixture was allowed to stir for 10 minutes and then cooled to 0 °C. Once cooled, a solution of DIAD (2.48 mL, 12.5 mmol) in THF (10 mL) was added to the reaction mixture over a period of 30 min. The mixture was allowed to reach to room temperature and was then stirred for 24 h. The mixture was concentrated under reduced pressure, and the residue was dissolved in Et_2O (30 mL). A solution of 2M NaOH (15 mL) was added, and the aqueous layer was extracted with Et_2O (3 × 10 mL). The combined organic extracts were washed with brine (15 mL), dried with $MgSO_4$, filtered and concentrated, and the residue was chromatographed on silica gel (2:3 EA/hexane) to yield the title compound as a colorless oil (1.00 g, 35%). R_f (50% EA/hex): 0.65. ^{1}H-NMR (400 MHz, $CDCl_3$) δ 7.79 – 7.77 (m, 2H), 7.72 – 7.60 (m, 3H), 7.27 – 7.08 (m, 2H), 7.08 – 6.95 (m, 4H), 6.73 (s, 1H), 5.49 (t, *J* = 7.8, 1H), 4.16 (dt, *J* = 10.0, 4.4, 1H), 3.79 (s, 2H), 3.70 (ddd, *J* = 13.1, 9.8, 3.5, 1H), 2.56 – 2.44 (m, 1H), 2.26 – 2.16 (m, 1H), 1.54 (s, 9H); ^{13}C-NMR (101 MHz, $CDCl_3$) δ 167.75, 153.57, 140.72, 137.40, 136.31, 134.14, 131.80, 128.78, 128.27, 127.87, 126.79, 126.40, 125.93, 124.50, 123.36, 80.98, 46.48, 43.20, 41.01, 28.51, 28.40.

(*S*)-*Tert*-butyl 4-amino-6-benzyl-3,4-dihydroquinoline-1(2*H*)-carboxylate (7): Compound **6** (933 mg, 1.99 mmol) was dissolved in absolute EtOH (20 mL) followed by the addition of hydrazine monohydrate (460 μL, 5.97 mmol). The reaction mixture was stirred at room temperature for 48 h, during which time a white precipitate formed. The mixture was filtered, the precipitate was washed with EtOH (20 mL), and the filtrate concentrated under reduced pressure. The residue was partitioned between EA (20 mL) and H_2O (10 mL), and the aqueous layer was extracted with EA (3 × 10 mL). Combined organic extracts were washed with brine (20 mL), dried with $MgSO_4$, filtered and concentrated under reduced pressure, and the residue was chromatographed on silica gel (1:9 MeOH/DCM) to yield the title compound as a colorless oil (240 mg, 60%, 78–80% ee). R_f (10% MeOH/DCM): 0.38. ^{1}H-NMR (400 MHz, $CDCl_3$) δ 7.62 (d, *J* = 8.5, 1H), 7.31 – 7.22 (m, 2H), 7.21 – 7.12 (m, 4H), 7.01 (dd, *J* = 8.5, 1.7, 1H), 3.92 (s, 2H), 3.90 (t, *J* = 5.8, 1H), 3.86 – 3.79 (m, 1H), 3.71 – 3.63 (m, 1H), 2.14 – 2.02 (m, 1H), 1.77 – 1.65 (m, 1H), 1.51 (s, 9H); ^{13}C-NMR (101 MHz, $CDCl_3$) δ 153.73, 141.13, 133.26, 128.87, 128.42, 127.44, 127.16, 126.02, 123.79, 80.89, 47.71, 41.57, 41.34, 33.21. Enantioselectivity determined by HPLC (Chiracel OD-RH column, 34% acetonitrile/water, 1.0 mL/min, 230 nm, 25 °C), t_{major} 4.79 min, t_{minor} 8.87 min.

General Procedure B for Compounds 8a–b

2-(4-Nitrophenyl)-1-phenylethanone (8a): To a mixture of p-nitrophenylacetic acid (19.5 g, 108 mmol) and 150 mL of benzene was added 25 g of the 1:1 P_2O_5/Al_2O_3 mixture. The reaction was stirred overnight at reflux and since starting material still could be seen by TLC, fresh P_2O_5/Al_2O_3 (10 g) was added and the reaction was kept under reflux and monitored by TLC until completion (6 h). The mixture was then filtered, concentrated, and suspended in 200 mL EA. The organic layer was washed with $NaHCO_3$ (3 × 50 mL) and brine (1 × 50 mL), dried over $MgSO_4$ and filtered. The crude residue was chromatographed on silica gel (1:1 EA/hex) to yield the title compound as a yellow solid (18 g, 70%). R_f (50% EA/hex): 0.70. ^{1}H NMR (500 MHz, $CDCl_3$) δ 8.22 (d, *J* = 8.6, 2H), 8.04 (d, *J* = 7.4, 2H), 7.64 (t, *J* = 7.4, 1H), 7.52 (dd, *J* = 10.5, 5.0, 2H), 7.46 (d, *J* = 8.4, 2H), 4.44 (s, 2H); ^{13}C-NMR (126 MHz, $CDCl_3$) δ 196.01, 142.07, 136.17, 133.76, 130.67, 130.52, 128.90, 128.45, 123.76, 77.32, 77.06, 76.81, 44.95.

Naphthalen-1-yl(4-nitrophenyl)methanone (8b): Synthesized according to general procedure A starting from p-nitrobenzoic acid (15.6 g, 93.0 mmol) and naphthalene (10.0 g, 78.0 mmol) using DCE (200 mL) as solvent to yield a yellow solid (19.0 g, 90%) as a 4:1 mixture of the title compound and the 2-naphthalene derivative, respectively. ^{1}H-NMR (500 MHz, $CDCl_3$) δ 8.34 – 8.28 (m, 2H), 8.20 – 8.15 (m, 1H), 8.07 (d, *J* = 8.1, 1H), 8.02 – 7.98 (m, 2H), 7.95 (dd, *J* = 6.8, 2.5, 1H), 7.63 – 7.49 (m, 4H); ^{13}C-NMR (126 MHz, $CDCl_3$) δ 195.98, 150.15, 143.30, 134.57, 133.77, 132.60, 131.12, 130.73, 128.95, 128.60, 127.86, 126.81, 125.33, 124.23, 123.60, 77.25, 77.00, 76.75.

Procedure for Compound 8c

2-(4-Nitrobenzyl)naphthalene (8c): 2-naphthalenyl boronic acid (1.29 g, 7.50 mmol) and p-nitrobenzyl bromide (1.25 g, 5.79 mmol) were added to a microwave vessel in 3:1 mixture of acetone/H_2O (7 mL) that was previously degassed and saturated with argon gas. $PdCl_2$ (17.4 mg, 1.69 mol%) and K_2CO_3 (2.40 g, 17.4 mmol) were then added. The mixture was irradiated at 110° C for 10 min. The suspension was then concentrated, suspended in DCM (50 mL), filtered through celite and chromatographed on silica gel (8:92 EA/hex) to yield the title compound as a beige solid (795 mg, 52%). R_f (8% EA/hex): 0.27. ^{1}H-NMR (400 MHz, $CDCl_3$) δ 8.13 (d, *J* = 8.6 Hz, 2H), 7.85 – 7.77 (m, 3H), 7.63 (s, 1H), 7.51 – 7.46 (m, 2H), 7.35 (d, *J* = 8.5 Hz, 2H), 7.27 (d, *J* = 8.2 Hz, 1H), 4.21 (s, 2H); ^{13}C-NMR (101 MHz,

$CDCl_3$) δ 148.69, 136.64, 133.59, 132.28, 129.72, 128.57, 128.25, 127.71, 127.56, 127.43, 127.21, 126.35, 125.82, 123.75, 77.39, 77.08, 76.76, 41.84.

Procedure for Compound 8d

2-(4-Nitrobenzylidene)-2,3-dihydro-1*H*-inden-1-one (8d): To a reaction vessel containing MeOH (375 mL) was added KOH (1.91 g, 34.0 mmol). After dissolution, 1-indanone (3.00 g, 22.7 mmol) was added and allowed to dissolve. p-nitrobenzaldehyde (4.12 g, 27.2 mmol) was then added to the reaction mixture and allowed to stir for 1 h. Solvent was removed under reduced pressure and the residual solid was washed with cold H_2O (50 mL) and filtered to yield a homogenous, tan powder (5.57 g, 93%). R_f (40% EA/hex): 0.42. ^{1}H-NMR (400 MHz, $CDCl_3$) δ 8.32 (d, *J* = 8.3, 2H), 7.94 (d, *J* = 7.7, 1H), 7.82 (d, *J* = 8.2, 2H), 7.73 – 7.63 (m, 2H), 7.59 (d, *J* = 7.5, 1H), 7.47 (t, *J* = 7.3, 1H), 4.10 (s, 2H); ^{13}C-NMR (101 MHz, $CDCl_3$) δ 193.63, 149.28, 147.68, 141.63, 138.43, 137.50, 135.26, 130.95, 130.81, 128.06, 126.24, 124.74, 124.08, 32.33.

General Procedure C for Compounds 9(a–d)

4-Phenethylaniline (9a): To a hydrogenation vessel was added 10% Pd/C catalyst (1.5 g) followed by the slow addition of MeOH (120 mL). **8a** (6.2 g, 25.7 mmol) was dissolved in minimal MeOH and added to the vessel, followed by conc. HCl (5.8 mL). The reaction vessel was placed on the hydrogenator uder 50 psi H_2 gas and allowed to shake for 24 h. The reaction mixture was then filtered through a pad of celite and solvent was removed under reduced pressure. The crude residue was extracted twice with DCM (150 mL) from 2M NaOH (200 mL) and the combined organic layers subsequently washed 2 × $NaHCO_3$ (100 mL), 1 × Brine (100 mL), dried under $MgSO_4$ filtered and concentrated. The crude residue was chromatographed on silica gel (4:1 EA/hex) to yield the title compound as a beige-pinkish solid (3.70 g, 73%). R_f (75% EA/hex): 0.54. ^{1}H-NMR (400 MHz, $CDCl_3$) δ 7.27 – 7.21 (m, 2H), 7.19 – 7.08 (m, 3H), 6.96 – 6.89 (m, 2H), 6.59 – 6.50 (m, 2H), 3.45 (d, *J* = 18.1, 2H), 2.84 (ddd, *J* = 8.7, 5.4, 2.2, 2H), 2.78 (ddd, *J* = 8.7, 5.4, 2.2, 2H); ^{13}C-NMR (101 MHz, $CDCl_3$) δ 144.16, 141.88, 131.64, 129.03, 128.33, 128.18, 128.11, 125.63, 115.06, 77.32, 77.00, 76.68, 38.11, 36.91.

4-(Naphthalenylmethyl)aniline (9b): was synthesized according to general procedure C starting from **8b** (10.0 g, 36.1 mmol) carrying over the 4:1 mixture of 1-napthalene and 2-napthalene intermediates, respectively, to yield a beige solid (8.00g, 95%). R_f (40% EA/hex): 0.40. ^{1}H-NMR (500 MHz, $CDCl_3$) δ 7.98 (dd, *J* = 8.6, 4.1, 1H), 7.83 – 7.79 (m, 1H), 7.70 (d, *J* = 8.5, 1H), 7.44 – 7.34 (m, 3H), 7.24 (d, *J* = 6.9, 1H), 6.94 (d, *J* = 8.3, 2H), 6.54 – 6.52 (m, 2H), 4.30 (s, 2H); ^{13}C-NMR (126 MHz, $CDCl_3$) δ 144.33, 137.29, 133.79, 132.04, 130.44, 129.47, 128.52, 126.97, 126.82, 125.77, 125.46, 125.40, 124.25, 115.21, 77.25, 77.00, 76.75, 38.08.

4-(Naphthalen-2-ylmethyl)aniline (9c): was synthesized according to general procedure C starting from **8c** (3.60 g, 13.7 mmol) to yield a beige solid (2.30 g, 70%). Rf (40% EA/hex): 0.40. ^{1}H-NMR (400 MHz, $CDCl_3$) δ 7.78 – 7.69 (m, 3H), 7.58 (s, 1H), 7.44 – 7.35 (m, 2H), 7.28 (dd, *J* = 8.4, 1.6 Hz, 1H), 6.98 (d, *J* = 8.3 Hz, 2H), 6.59 – 6.56 (m, 2H), 4.00 (s, 2H), 3.43 (d, *J* = 42.6 Hz, 2H); ^{13}C-NMR (101 MHz, $CDCl_3$) δ 144.49, 139.34, 133.53, 131.93, 130.86, 129.76, 127.85, 127.57, 127.50, 127.44, 126.73, 125.79, 125.11, 115.22, 77.32, 77.00, 76.68, 41.15.

4-((2,3-dihydro-1*H*-inden-2-yl)methyl)aniline (9d): was synthesized according to general procedure C starting from **8d** (2.13 g, 8.04 mmol) to yield a brown solid (1.70 g, 95%). R_f (5% MeOH/DCM): 0.78. ^{1}H-NMR (400 MHz, $CDCl_3$) δ 7.16 (dd, *J* = 8.0, 4.5, 2H), 7.14 – 7.08 (m, 2H), 7.01 (d, *J* = 8.2, 2H), 6.67 (d, *J* = 8.2, 2H), 3.31 (s, 2H), 2.97 (dd, *J* = 13.7, 5.7,

2H), 2.75 – 2.60 (m, 5H); ^{13}C-NMR (101 MHz, $CDCl_3$) δ 143.34, 131.97, 129.67, 126.04, 124.48, 115.51, 41.71, 40.73, 38.86.

General Procedure D for Compounds 10(a–d)

3-Bromo-*N*-(4-phenethylphenyl)propanamide (10a): Compound **9a** (587 mg, 2.90 mmol) was added to a suspension of K_2CO_3 (820 mg, 5.94 mmol) in DCM (10 mL), followed by the addition of 3-bromopropionyl chloride (300 μL, 2.99 mmol) via syringe. The resulting mixture was stirred at room temperature for 2 h and quenched by the addition of H_2O (10 mL). The mixture was extracted with DCM (25 mL), dried with $MgSO_4$, filtered and concentrated to yield the title compound as a tan solid (921 mg, 93%). R_f (75% EA/hex): 0.70. ^{1}H-NMR (400 MHz, $CDCl_3$) δ 7.48 (s, 1H), 7.43 – 7.39 (m, 2H), 7.29 – 7.24 (m, 2H), 7.21 – 7.09 (m, 5H), 3.68 (t, *J* = 6.6, 2H), 2.90 (t, *J* = 6.6, 2H), 2.89 (s, 4H); ^{13}C-NMR (101 MHz, $CDCl_3$) δ 167.91, 141.51, 138.24, 135.27, 128.95, 128.41, 128.29, 125.89, 120.21, 77.32, 77.00, 76.68, 40.55, 37.82, 37.24, 27.15.

3-Bromo-*N*-(4-(naphthalen-1-ylmethyl)phenyl)propanamide (10b): was synthesized according to general procedure D starting from **9b** (1.40 g, 6.00 mmol). The crude compound was chromatographed on silica gel (4:1 EA/hex) to yield the title compound as a tan solid (1.00 g, 45%). R_f (75% EA/hex): 0.72. ^{1}H-NMR (400 MHz, $CDCl_3$) δ 7.96 – 7.91 (m, 1H), 7.83 (dt, *J* = 4.1, 2.8, 1H), 7.74 (dd, *J* = 8.0, 4.4 Hz, 1H), 7.42 – 7.35 (m, 3H), 7.25 (d, *J* = 6.9), 7.12 (d, *J* = 8.5, 1H), 4.38 (s, 2H), 3.63 (t, *J* = 6.6, 2H), 2.85 (t, *J* = 6.5, 2H); ^{13}C-NMR (101 MHz, $CDCl_3$) δ 167.92, 137.11, 136.41, 135.38, 133.89, 131.98, 129.20, 128.64, 127.25, 127.18, 125.96, 125.55, 125.50, 124.16, 120.34, 77.32, 77.00, 76.68, 40.50, 38.46, 27.11.

3-Bromo-*N*-(4-(naphthalen-2-ylmethyl)phenyl)propanamide (10c): was synthesized according to general procedure D starting from **9c** (2.20 g, 9.00 mmol) to yield the title compound as a beige solid (3.30 g, 90%). R_f (75% EA/hex): 0.71. ^{1}H-NMR (400 MHz, $CDCl_3$) δ 7.81 – 7.72 (m, 2H), 7.60 (s, 1H), 7.50 – 7.34 (m, 4H), 7.31 – 7.23 (m, 1H), 7.18 (d, *J* = 8.2, 2H), 7.12 (d, *J* = 8.1, 1H), 4.09 (s, 2H), 3.68 (t, *J* = 6.6, 2H), 2.90 (t, *J* = 6.5, 2H); ^{13}C-NMR (101 MHz, $CDCl_3$) δ 167.85, 138.45, 137.43, 135.52, 133.56, 132.06, 129.57, 128.09, 127.59, 127.51, 127.00, 125.99, 125.36, 120.31, 120.20, 77.32, 77.00, 76.68, 41.48, 40.61, 27.09.

3-Bromo-*N*-(4-((2,3-dihydro-1H-inden-2-yl)methyl)phenyl)propanamide (10d): was synthesized according to general procedure D starting from **9d** (686 mg, 3.07 mmol) to yield the title compound as a fluffy, white solid (1.07 g, 98%). R_f (40% EA/hex): 0.37. ^{1}H-NMR (400 MHz, $CDCl_3$) δ 7.44 (d, *J* = 8.2, 2H), 7.20-7.06 (m, 6H), 3.71 (t, *J* = 6.5, 2H), 2.98 – 2.63 (m, 4H), 2.77 – 2.60 (m, 5H); ^{13}C-NMR (101 MHz, $CDCl_3$) δ 167.74, 143.10, 137.96, 135.21, 129.39, 126.11, 124.48, 120.13, 41.46, 40.93, 40.69, 38.81, 27.16.

General Procedure E for Compounds 11(a–d)

1-(4-Phenethylphenyl)azetidin-2-one (11a): NaO*t*Bu (269 mg, 2.8 mmol) was suspended in DMF (20 mL) followed by the addition of **10a** (883 mg, 2.66 mmol) previously dissolved in DMF (10 mL) via cannula. The resulting mixture was stirred at room temperature for 3 h, quenched with H_2O (10 mL), and concentrated under reduced pressure to an oil which was resuspended in EA (20 mL) and washed with H_2O (2 × 20 mL), brine (1 × 20 mL), dried with $MgSO_4$, filtered and concentrated, and chromatographed on silica gel (1:1 EA/hex) to yield the title compound as a white solid (457 mg, 70%). R_f (50% EA/hex): 0.49. ^{1}H-NMR (400 MHz, $CDCl_3$) δ 7.29 – 7.23 (m, 4H), 7.21 – 7.09 (m, 5H), 3.59 (t, *J* = 4.4, 2H), 3.08 (t, *J* = 4.5, 2H), 2.88 (s, 4H); ^{13}C-NMR (101 MHz, $CDCl_3$) δ 164.25, 141.47, 137.27, 136.55,

129.07, 128.43, 128.27, 125.89, 116.08, 77.32, 77.00, 76.68, 37.96, 37.91, 37.30, 36.00, 28.09.

1-(4-(Naphthalen-1-ylmethyl)phenyl)azetidin-2-one (11b): was synthesized according to general procedure E starting from **10b** (1.00 g, 2.71 mmol) to yield the title compound as a yellow solid (603 mg, 77%). R_f (50% EA/hex): 0.38. ^{1}H-NMR (400 MHz, $CDCl_3$) δ 7.94 (dd, *J* = 6.3, 3.0, 1H), 7.84 (dd, *J* = 6.1, 3.2, 1H), 7.74 (dd, *J* = 8.3, 3.6, 1H), 7.45 – 7.39 (m, 3H), 7.24 (dd, *J* = 7.8, 6.0, 3H), 7.14 (d, *J* = 8.4, 2H), 4.38 (s, 2H), 3.50 (t, *J* = 4.5, 2H), 3.02 (t, *J* = 4.5, 2H); ^{13}C-NMR (101 MHz, $CDCl_3$) δ 164.21, 136.64, 136.49, 136.11, 133.88, 131.95, 129.31, 128.62, 127.15, 125.92, 125.52, 125.47, 124.11, 116.20, 77.32, 77.00, 76.68, 38.49, 37.90, 35.97.

1-(4-(Naphthalen-2-ylmethyl)phenyl)azetidin-2-one (11c): was synthesized according to general procedure E starting from **10c** (3.20 g, 8.70 mmol) to yield the title compound as a yellow solid (2.30g, 90%). R_f (50% EA/hex): 0.32. ^{1}H-NMR (400 MHz, $CDCl_3$) δ 7.80 – 7.71 (m, 3H), 7.58 (s, 1H), 7.42 (dt, *J* = 13.7, 6.8, 2H), 7.26 (dd, *J* = 12.8, 6.0, 2H), 7.21 – 7.09 (m, 3H), 4.09 (s, 2H), 3.56 (t, *J* = 4.2, 2H), 3.06 (t, *J* = 4.4, 2H); ^{13}C-NMR (101 MHz, $CDCl_3$) δ 164.32, 138.51, 136.73, 136.50, 133.54, 132.03, 129.67, 128.07, 127.57, 127.48, 127.41, 126.92, 125.97, 125.34, 116.28, 77.32, 77.00, 76.68, 41.49, 37.98, 36.00.

1-(4-((2,3-Dihydro-1*H*-inden-2-yl)methyl)phenyl)azetidin-2-one (11d): was synthesized according to general procedure E starting from **10d** (1.07 g, 3.00 mmol) to yield the title compound as a light tan powder (811 mg, 98%). R_f (40% EA/hex): 0.37. ^{1}H-NMR (400 MHz, $CDCl_3$) δ 7.31 (d, *J* = 8.3, 2H), 7.20-7.09 (m, 6H), 3.62 (t, *J* = 4.4, 2H), 3.11 (t, *J* = 4.4, 2H), 2.97 (dd, *J* = 14.6, 5.4, 2H), 2.78-2.61 (m, 5H); ^{13}C-NMR (400 MHz, $CDCl_3$) δ 164.26, 143.10, 137.03, 136.61, 129.47, 126.14, 124.49, 116.16, 41.56, 41.00, 38.82, 38.01, 36.07.

General Procedure F for Compounds 12(a–d)

6-Phenethyl-2,3-dihydroquinolin-4(1*H*)-one (12a): Compound **11a** (424mg, 1.68 mmol) was dissolved in DCE (50 mL) and TfOH (448 μL, 5.06 mmol) was added via syringe. The resulting mixture was stirred at room temperature for 18 h, then quenched with K_2CO_3 (1.7 g) and H_2O (86 μL), and allowed to stir for 1 h. The mixture was filtered through a plug of $MgSO_4$, and concentrated under reduced pressure to yield the title compound as a yellow solid (338mg, 80%). R_f (70% EA/hex): 0.49. ^{1}H-NMR (400 MHz, $CDCl_3$) δ 7.72 – 7.71 (m, 1H), 7.30 – 7.25 (m, 2H), 7.21 – 7.14 (m, 3H), 7.10 (dd, *J* = 8.4, 2.2, 1H), 6.60 (d, *J* = 8.3, 1H), 4.65 – 3.78 (bs, 1H), 3.55 (dd, *J* = 7.4, 6.5, 2H), 2.91 – 2.78 (m, 4H), 2.69 (dd, *J* = 7.4, 6.5, 2H); ^{13}C-NMR (101 MHz, $CDCl_3$) δ 193.83, 150.38, 141.62, 135.78, 131.42, 128.41, 128.30, 126.66, 125.87, 119.33, 115.89, 77.30, 76.99, 76.67, 42.45, 38.18, 37.94, 36.88.

6-(Naphthalen-1-ylmethyl)-2,3-dihydroquinolin-4(1*H*)-one (12b): was synthesized according to general procedure F starting from **11b** (603 mg, 2.10 mmol) to yield the title compound as a yellow solid (450 mg, 74%). R_f (50% EA/hex): 0.43. ^{1}H NMR (400 MHz, $CDCl_3$) δ 8.00 – 7.95 (m, 1H), 7.84 – 7.79 (m, 1H), 7.77 (d, *J* = 1.8, 1H), 7.71 (d, *J* = 7.9, 1H), 7.44 – 7.35 (m, 3H), 7.26 (d, *J* = 6.5, 1H), 7.05 (dd, *J* = 8.4, 2.1, 1H), 6.49 (d, *J* = 8.4, 1H), 4.29 (s, 2H), 3.46 (t, *J* = 7.04, 2H), 2.63 (t, *J* = 6.88, 2H); ^{13}C-NMR (101 MHz, $CDCl_3$) δ 193.78, 150.54, 136.60, 135.66, 133.89, 131.92, 130.10, 128.62, 127.24, 127.13, 127.10, 127.07, 125.92, 125.49, 124.10, 119.16, 116.13, 77.32, 77.00, 76.68, 42.28, 38.10, 38.02.

6-(Naphthalen-2-ylmethyl)-2,3-dihydroquinolin-4(1*H*)-one (12c): was synthesized according to general procedure F starting from **11c** (2.30 g, 8.01 mmol) to yield the title compound as a yellow solid (1.40 g, 61%). R_f (50% EA/hex): 0.43. ^{1}H-NMR (400 MHz,

CDCl3) δ 7.80 – 7.70 (m, 4H), 7.60 (s, 1H), 7.46 – 7.38 (m, 2H), 7.28 (d, *J* = 8.4, 1H), 7.14 – 7.09 (m, 1H), 6.54 (d, *J* = 8.4, 1H), 4.36 (s, 1H), 4.00 (s, 2H), 3.45 (t, *J* = 6.9, 2H), 2.64 (t, *J* = 6.9, 2H); ^{13}C-NMR (101 MHz, $CDCl_3$) δ 193.80, 150.64, 138.65, 136.04, 133.48, 131.96, 130.35, 128.01, 127.50, 127.43, 127.33, 127.13, 126.75, 125.87, 125.23, 118.99, 116.22, 77.32, 77.00, 76.68, 42.16, 41.02, 38.00.

6-((2,3-Dihydro-1*H*-inden-2-yl)methyl)-2,3-dihydroquinolin-4(1*H*)-one (12d): was synthesized according to general procedure F starting from **11d** (811 mg, 2.93 mmol) to yield the title compound as a viscous yellow oil (772 mg, 95%). R_f (40% EA/hex): 0.32. ^{1}H-NMR (400 MHz, $CDCl_3$) δ 7.70 (d, *J* = 1.9, 1H), 7.22 – 7.08 (m, 5H), 6.63 (d, *J* = 8.3, 1H), 4.30 (br s, 1H), 3.57 (t, *J* = 6.9, 2H), 2.97 (dd, *J* = 14.2, 5.9, 2H), 2.78 – 2.60 (m, 7H); ^{13}C-NMR (101 MHz, $CDCl_3$) δ 193.84, 150.42, 143.12, 136.09, 131.00, 127.12, 126.06, 124.45, 119.30, 115.90, 42.47, 41.42, 40.42, 38.75, 38.22.

General Procedure G for Compounds 13(a–d)

(*E/Z*)-6-Phenethyl-2,3-dihydroquinolin-4(1*H*)-one oxime (13a): Compound **12a** (338 mg, 1.35 mmol) was suspended in 1:1 EtOH/H_2O followed by the addition of $NH_2OH{\cdot}HCl$ (64.5 mg, 1.47 mmol) and $NaOAc{\cdot}H_2O$ (201 mg, 1.47 mmol). The mixture was stirred at reflux overnight, after which time solvents were condensed and redissolved in EA (30 mL). The organic layer was washed with brine (10 mL), dried with $MgSO_4$, filtered, concentrated under reduced pressure and chromatographed on silica gel (1:1 EA/hex) to yield the title compound as a yellow solid (235 mg, 66%). R_f (50% EA/hex): 0.51 ^{1}H-NMR (400 MHz, $CDCl_3$) δ 7.66 (d, *J* = 2.0, 1H), 7.29 – 7.23 (m, 2H), 7.20 – 7.14 (m, 3H), 6.95 (dd, *J* = 8.2, 2.1, 1H), 6.57 – 6.52 (m, 1H), 3.30 (t, *J* = 6.5, 2H), 2.93 (t, *J* = 6.5, 2H), 2.90 – 2.76 (m, 4H); ^{13}C-NMR (101 MHz, $CDCl_3$) δ 152.47, 145.29, 141.92, 131.99, 130.95, 128.42, 128.27, 125.78, 123.71, 116.68, 115.85, 77.32, 77.00, 76.68, 40.71, 38.09, 37.16, 23.58.

(*E/Z*)-6-(Naphthalen-1-ylmethyl)-2,3-dihydroquinolin-4(1*H*)-one oxime (13b): was synthesized according to general procedure G starting from **12b** (450 mg, 1.57 mmol) and chromatographed on silica gel (4:1 EA/hex) to yield the title compound as a yellow solid (313 mg, 66%). R_f (75% EA/hex): 0.73. ^{1}H-NMR (400 MHz, $CDCl_3$) δ 8.02 – 7.97 (m, 1H), 7.83 – 7.77 (m, 1H), 7.70 (s, 2H), 7.41 (m, 3H), 7.26 – 7.21 (m, 1H), 6.85 (dt, *J* = 11.2, 5.6, 1H), 6.42 (d, *J* = 8.3, 1H), 4.28 (s, 2H), 3.17 (t, *J* = 6.4, 2H), 2.85 (t, *J* = 5.2, 2H); ^{13}C-NMR (101 MHz, $CDCl_3$) δ 152.20, 145.35, 133.83, 130.94, 130.52, 129.49, 128.53, 127.02, 126.87, 125.85, 125.49, 125.41, 124.24, 124.20, 116.68, 115.98, 115.48, 77.32, 77.00, 76.68, 40.55, 38.18, 23.51.

(*E/Z*)-6-(Naphthalen-2-ylmethyl)-2,3-dihydroquinolin-4(1*H*)-one oxime (13c): was synthesized according to general procedure G starting from **12c** (522 mg, 1.81 mmol) to yield the title compound as a yellow solid (453 mg, 82%). R_f (50% EA/hex): 0.51. ^{1}H-NMR (400 MHz, $CDCl_3$) δ 7.77 – 7.61 (m, 3H), 7.56 (d, *J* = 9.2, 1H), 7.42 – 7.32 (m, 2H), 7.26 (dd, *J* = 8.4, 1.3, 1H), 6.92 (dt, *J* = 6.8, 3.5, 1H), 6.50 (d, *J* = 8.3, 1H), 3.97 (s, 2H), 3.28 – 3.20 (m, 2H), 2.84 (t, *J* = 6.5, 2H); ^{13}C-NMR (101 MHz, $CDCl_3$) δ 152.40, 145.46, 139.04, 133.58, 132.01, 131.37, 131.08, 127.99, 127.57, 127.55, 126.86, 125.83, 125.18, 124.46, 116.67, 116.06, 115.81, 77.32, 77.00, 76.68, 41.36, 40.64, 23.41.

(*E/Z*)-6-((2,3-Dihydro-1*H*-inden-2-yl)methyl)-2,3-dihydroquinolin-4(1*H*)-one oxime (13d): was synthesized according to general procedure G starting from **12d** (772 mg, 2.78 mmol) to yield the title compound as a yellow solid (662 mg, 81%). R_f (40% EA/hex): 0.44. ^{1}H NMR (400 MHz, $CDCl_3$) 7.63 (d, *J* = 1.8, 1H), 7.19 –7.05 (m, 5H), 6.60 (dd, *J* = 21.6, 8.3, 1H), 3.30 (t, *J* = 6.5, 2H), 2.93 (dt, *J* = 13.0, 7.6, 3H), 2.76 – 2.59 (m, 6H); ^{13}C

NMR (101 MHz, $CDCl_3$) δ 152.50, 145.41, 143.38, 131.51, 131.34, 129.41, 126.08, 124.52, 124.23, 115.78, 41.57, 40.78, 40.74, 38.86, 23.45.

General Procedure H for Compounds 14(a–d)

6-Phenethyl-1,2,3,4-tetrahydroquinolin-4-amine (14a): 10% Pd/C (50 mg) was added to a hydrogenation vessel followed by the slow addition of MeOH (10 mL). **13a** (170 mg, 0.64 mmol) was dissolved in minimal MeOH and added to the vessel, followed by the addition of glacial AcOH (0.4 mL). The reaction vessel was placed on the hydrogenator under 40 psi H_2 gas and allowed to shake for 12 h. The reaction mixture was then filtered through a pad of celite, and solvent was removed under reduced pressure. The crude residue was resuspended in 1M HCl (30 mL) and extracted with 3 × EA (30 mL). The organic layer was washed with 3 × 2M NaOH (30 mL), 1 × Brine (30 mL), dried under $MgSO_4$ filtered and concentrated, to yield the title compound as a tan oil (120 mg, 75%), which was carried to the next reaction without further purification. ^{1}H-NMR (400 MHz, $CDCl_3$) δ 8.61 (bs, 2H), 7.28 – 7.20 (m, 3H), 7.16 (dd, *J* = 13.2, 7.1, 3H), 6.82 (d, *J* = 8.3, 1H), 6.38 (d, *J* = 8.2, 1H), 4.33 (s, 1H), 3.45 (t, *J* = 11.2, 1H), 3.14 (dd, *J* = 8.2, 4.0, 1H), 2.86 – 2.77 (m, 2H), 2.74 – 2.68 (m, 2H), 2.24 (d, *J* = 12.2, 1H), 2.12 – 2.03 (m, 1H); ^{13}C-NMR (101 MHz, $CDCl_3$) δ 143.00, 141.99, 131.01, 130.37, 130.15, 128.49, 128.25, 125.77, 115.30, 115.03, 77.33, 77.01, 76.69, 47.35, 38.16, 36.96, 36.61, 26.38. ESI-MS 236.1 $[M\text{-}NH_3+H]^+$. HPLC (gradient A): retention time = 23.79 min.

6-(Naphthalen-1-ylmethyl)-1,2,3,4-tetrahydroquinolin-4-amine (14b): was synthesized according to general procedure H starting from **13b** (330 mg, 1.09 mmol) to yield the title compound as a tan oil (253 mg, 84%). ^{1}H-NMR (400 MHz, $CDCl_3$) δ 8.00 (d, *J* = 7.9, 1H), 7.81 (d, *J* = 7.5, 1H), 7.69 (d, *J* = 8.0, 1H), 7.44 – 7.39 (m, 2H), 7.36 (s, 1H), 7.27 – 7.21 (m, 1H), 7.19 (s, 1H), 6.79 (d, *J* = 7.9, 1H), 6.31 (d, *J* = 8.2, 1H), 5.06 (bs, 3H), 4.24 (s, 2H), 4.08 (s, 1H), 3.44 – 3.29 (m, 1H), 3.14 (m, 1H), 2.00 (s, 2H); ^{13}C-NMR (101 MHz, $CDCl_3$) δ 142.75, 137.30, 133.83, 132.04, 129.94, 129.58, 129.23, 128.55, 127.53, 127.04, 126.84, 125.91, 125.55, 125.44, 124.31, 115.00, 77.32, 77.00, 76.68, 46.97, 38.00, 37.00, 28.34. ESI-MS 272.1 $[M\text{-}NH_3+H]^+$. HPLC (gradient A): retention time = 31.71 min.

6-(Naphthalen-2-ylmethyl)-1,2,3,4-tetrahydroquinolin-4-amine (14c): was synthesized according to general procedure H starting from **13c** (618 mg, 2.04 mmol) to yield the title compound as a tan oil (246 mg, 86%). ^{1}H-NMR (400 MHz, CD_3OD) δ 7.75 (dd, *J* = 15.5, 8.4, 3H), 7.62 (s, 1H), 7.41 (dt, *J* = 12.8, 6.3, 2H), 7.31 (d, *J* = 8.2, 1H), 7.14 (s, 1H), 7.07 (d, *J* = 8.0, 1H), 6.67 (d, *J* = 8.2, 1H), 4.42 (t, *J* = 4.5, 1H), 4.02 (s, 2H), 3.40 – 3.31 (m, 2H), 2.26 – 2.03 (m, 2H); ^{13}C-NMR (101 MHz, CD_3OD) δ 143.71, 140.64, 135.10, 133.55, 132.32, 132.09, 130.74, 128.96, 128.56, 128.49, 128.47, 127.75, 126.99, 126.32, 117.45, 49.64, 49.43, 49.21, 49.00, 48.79, 48.57, 48.36, 48.01, 42.09, 37.45, 27.37. ESI-MS 272.1 $[M\text{-}NH_3+H]^+$. HPLC (gradient A): retention time = 34.07 min.

6-((2,3-Dihydro-1*H*-inden-2-yl)methyl)-1,2,3,4-tetrahydroquinolin-4-amine (14d): was synthesized according to general procedure H starting from **13d** (662 mg, 2.26 mmol) to yield the title compound as a brown oil (527 mg, 84%). ^{1}H-NMR (400 MHz, $CDCl_3$) 7.13 (ddd, *J* = 8.7, 7.0, 4.2, 5H), 7.05 (s, 1H), 6.87 (dd, J=8.1, 1.8, 1H) 6.46 (t, *J* = 6.8, 1H), 4.00 (t, *J* = 4.8, 1H), 3.43 – 3.34 (m, 1H), 3.29 (dt, *J* = 11.0, 5.4, 1H), 3.02 – 2.94 (m, 3H), 2.77 – 2.59 (m, 6H); ^{13}C-NMR (101 MHz, $CDCl_3$) δ 157.04, 150.14, 143.38, 130.14, 129.11, 128.42, 125.98, 124.44, 114.50, 46.89, 41.70, 40.74, 38.88, 37.75, 31.65. ESI-MS 262.1 $[M\text{-}NH_3+H]^+$. HPLC (gradient A): retention time = 31.39 min.

General Procedure for Compounds 15(a–d)

(2*S*)-2-Amino-3-(4-hydroxy-2,6-dimethylphenyl)-*N*-(6-phenethyl-1,2,3,4-tetrahydroquinolin-4-yl)propanamide (15a): was synthesized according to general procedure A from **14a** (94 mg, 0.37 mmol) to yield 150 mg of crude diastereomers which were isolated by semipreparative HPLC and lyophilized to give white fluffy powders. HPLC (gradient A): retention time = 25.00 min (early), 28.19 min (late). ESI-MS 466.1 $[M+Na]^+$ for both diastereomers.

(2*S*)-2-Amino-3-(4-hydroxy-2,6-dimethylphenyl)-*N*-(6-(naphthalen-1-ylmethyl)-1,2,3,4-tetrahydroquinolin-4-yl)propanamide (15b): was synthesized according to general procedure A from **14b** (253 mg, 0.88 mmol) to yield 350 mg of a crude mixture of 1-napthalene and 2-napthalene derivatives as diastereomers. Only the earliest eluting peak was isolated as a pure compound by semipreparative HPLC to give a white powder. HPLC (gradient A): retention time = 31.42 min (early), 33.93 min (late). Confirmed by NMR to be the 1-napthalene derivative. ESI-MS 502.1 $[M+Na]^+$ for both diastereomers.

(2*S*)-2-Amino-3-(4-hydroxy-2,6-dimethylphenyl)-*N*-(6-(naphthalen-2-ylmethyl)-1,2,3,4-tetrahydroquinolin-4-yl)propanamide (15c): was synthesized according to general procedure A from **14c** (127 mg, 0.44 mmol) to yield 200 mg of a crude mixture of diastereomers which were isolated and purified by semipreparative HPLC, then lyophilized to give white powders. HPLC (gradient A): retention time = 32.44 min (early), 34.75 min (late). ESI-MS 502.2 $[M+Na]^+$ for both diastereomers.

(2*S*)-1-((6-((2,3-Dihydro-1*H*-inden-2-yl)methyl)-1,2,3,4-tetrahydroquinolin-4-yl)amino)-3-(4-hydroxy-2,6-dimethylphenyl)-1-oxopropan-2-amide (15d): was synthesized according to general procedure A from **14d** as a mixture of crude diastereomers which were isolated and purified by semipreparative HPLC and lyophilized to give a white powder of the early diastereomer and a tan powder of the late diastereomer. HPLC (gradient A): retention time = 31.09 min (early), 33.76 min (late). ESI-MS 492.2 $[M+Na]^+$ for both diastereomers.

In vitro pharmacology

Cell Lines and Membrane Preparations—All tissue culture reagents were purchased from Gibco Life Sciences (Grand Island, NY, USA). C6-rat glioma cells stably transfected with a rat mu (C6-MOR) or rat delta (C6-DOR) opioid receptor[20] and Chinese hamster ovary (CHO) cells stably expressing a human kappa (CHO-KOR) opioid receptor[21] were used for all *in vitro* assays. Cells were grown to confluence at 37°C in 5% CO_2 in Dulbecco's Modified Eagle's Medium containing 10% fetal bovine serum and 5% penicillin/streptomycin. Membranes were prepared by washing confluent cells three times with ice cold phosphate-buffered saline (0.9% NaCl, 0.61 mM Na_2HPO_4, 0.38 mM KH_2PO_4, pH 7.4). Cells were detached from the plates by incubation in warm harvesting buffer (20 mM HEPES, 150 mM NaCl, 0.68 mM EDTA, pH 7.4) and pelleted by centrifugation at 200×g for 3 min. The cell pellet was suspended in ice-cold 50 mM Tris-HCl buffer, pH 7.4 and homogenized with a Tissue Tearor (Biospec Products, Inc, Bartlesville, OK, USA) for 20 s at setting 4. The homogenate was centrifuged at 20,000×g for 20 min at 4 °C, and the pellet was rehomogenized in 50 mM Tris-HCl with a Tissue Tearor for 10 s at setting 2, followed by recentrifugation. The final pellet was resuspended in 50mM Tris-HCl and frozen in aliquots at 80 °C. Protein concentration was determined via Bradford assay using bovine serum albumin as the standard.

Radioligand Binding Assays—Radioactive compounds were purchased from Perkin-Elmer (Waltham, MA, USA). Opioid ligand-binding assays were performed using

competitive displacement of 0.2 nM [^{3}H]diprenorphine (250 μCi, 1.85 TBq/mmol) by the test compound from membrane preparations containing opioid receptors. The assay mixture, containing membrane suspension (20 μg protein/tube) in 50 mM Tris-HCl buffer (pH 7.4), [^{3}H]diprenorphine, and various concentrations of test peptide, was incubated at room temperature for 1 h to allow binding to reach equilibrium. The samples were rapidly filtered through Whatman GF/C filters using a Brandel harvester (Brandel, Gaithersburg, MD, USA) and washed three times with 50 mM Tris-HCl buffer. The radioactivity retained on dried filters was determined by liquid scintillation counting after saturation with EcoLume liquid scintillation cocktail in a Wallac 1450 MicroBeta (Perkin-Elmer, Waltham MA, USA). Nonspecific binding was determined using 10 μM naloxone. K_i values were calculated using nonlinear regression analysis to fit a logistic equation to the competition data using GraphPad Prism version 5.01 for Windows (GraphPad Software Inc, La Jolla, CA). The results presented are the mean ± standard error from at least three separate assays performed in duplicate.

Stimulation of [^{35}S]GTPγS Binding—Agonist stimulation of [^{35}S] guanosine 5′-O-[gamma-thio]triphosphate ([^{35}S]GTPγS, 1250 Ci, 46.2 TBq/mmol) binding was measured as described previously[22]. Briefly, membranes (10–20 μg of protein/tube) were incubated 1 h at room temperature in GTPγS buffer (50 mM Tris-HCl, 100 mM NaCl, 5 mM $MgCl_2$, pH 7.4) containing 0.1 nM [^{35}S]GTPγS, 30 μM guanosine diphosphate (GDP), and varying concentrations of test peptides. Peptide stimulation of [^{35}S]GTPγS was compared with 10 μM standard compounds [D-Ala^2, N-MePhe^4, Gly-ol]-enkephalin (DAMGO) at MOR, D-Pen^{2,5}-enkephalin (DPDPE) at DOR, or U69,593 at KOR. The reaction was terminated by rapidly filtering through GF/C filters and washing ten times with GTPγS buffer, and retained radioactivity was measured as described above. The results presented are the mean ± standard error from at least three separate assays performed in duplicate; maximal stimulation was determined using nonlinear regression analysis with GraphPad Prism (GraphPad Software Inc, La Jolla, CA).

In vivo pharmacology

Animals—Adult male C57BL/6 mice weighing between 20–30 g at 8–16 weeks old were used for the current experiments (obtained from Jackson Laboratories (Bar Harbor, Maine), Harlan (Indianapolis, IN), or bred in-house). Mice were group-housed and had free access to food and water at all times. Experiments were conducted in the housing room, which was maintained on a 12 h light/dark cycle (with lights on at 0700). Each mouse was used only once and experiments were conducted between 11 am and 4 pm. Studies were performed in accordance with the University of Michigan Committee on the Use and Care of Animals and the Guide for the Care and Use of Laboratory Animals (National Research Council, 2011 publication).

Antinociception—The antinociceptive effects of **1**(*4R*) and morphine were evaluated in the warm water tail withdrawal assay using a cumulative dosing procedure[23]. To determine tail withdrawal latencies, each mouse was placed briefly into a plastic, cylindrical restrainer and 2–3 cm of the tail tip was placed into a water bath maintained at 50 °C. The latency to withdraw the tail was recorded with a maximum cutoff time of 20 sec. If the mouse did not remove its tail by the cutoff time, the experimenter removed its tail from the water to prevent tissue damage. Each animal received an injection of saline (intraperitoneal; ip) and then 30 min later, the baseline withdrawal latencies were recorded and ranged between 3–6 sec. Following baseline determinations, three increasing doses (1, 2.2, and 6.8 mg/kg) of **1**(*4R*) were given in 30 min intervals to provide final doses of 1, 3.2 and 10 mg/kg. Thirty min after each injection, the tail withdrawal latency was measured as described above. To confirm **1**(*4R*) was acting at opioid receptors the cumulative dose response was repeated

over the dose-range 3.2, 10 and 32mg/kg following a 30 min pretreatment with 1 mg/kg naltrexone (ip). To determine the time-course of antinociceptive action the tail-withdrawal test was performed at varying times following administration of morphine (10 mg/kg, ip) or **1**(*4R*) (10 mg/kg, ip).

Acknowledgments

This work was funded by NIH grants DA003910 (H.I.M.) and DA004087 (J.R.T.). J.P.A. was supported by NIH predoctoral training grants DA007281 and GM007767. L.Y. was supported by NIH postdoctoral training grant DA007267. AAH was supported by NIH predoctoral training grant DA007281 and by a University of Michigan College of Pharmacy Lyons Fellowship.

Abbreviations used

MOR	mu opioid receptor
DOR	delta opioid receptor
KOR	kappa opioid receptor
Aic	2-amino indane, 2-carboxylic acid
Pen	penicillamine
cSEtS	cyclization through an ethylene dithioether linkage
cSS	cyclization through a disulfide linkage
THQ	tetrahydroquinoline
CHO	Chinese hamster ovary
GTPγS	guanosine 5′-*O*-[gamma-thio]triphosphate
WWTW	warm water tail withdrawal
TM	transmembrane
1-Nal	1-naphthylalanine
2-Nal	2-naphthylalanine
$(Boc)_2O$	di-*tert*-butyl dicarbonate
DIEA	N,N-diisopropylethylamine
EA	ethyl acetate
hex	hexanes
DIAD	diisopropylazodicarboxylate
TfOH	triflic acid
PyBOP	benzotriazol-1-yl-oxytripyrrolidinophosphonium hexafluorophosphate
HOBt-Cl	6-chloro hydroxybenzotriazole
Boc-Dmt	Boc-protected 2,6-dimethyl tyrosine

References

1. Morphy R, Kay C, Rankovic Z. From Magic Bullets to Designed Multiple Ligands. Res Focus Rev. 2004; 9:641–652.
2. Morphy R, Rankovic Z. Designing Multiple Ligands - Medicinal Chemistry Strategies and Challenges. Curr Pharmaceut Des. 2009; 15:587–600.

3. Morphy R, Rankovic Z. Designed multiple ligands. An emerging drug discovery paradigm. J Med Chem. 2005; 48:6523–6543. [PubMed: 16220969]
4. Abdelhamid EE, Sultana M, Portoghese PS, Takemori AE. Selective Blockage of the Delta Opioid Receptors Prevents the Development of Morphine Tolerance and Dependence in Mice. J Pharmacol Exp Ther. 1991; 258:299–303. [PubMed: 1649297]
5. Fundytus ME, Schiller PW, Shapiro M, Weltrowska G, Coderre TJ. Attenuation of Morphine Tolerance and Dependence with the Highly Selective Delta Opioid Receptor Antagonist TIPP(psi). Eur J Pharmacol. 1995; 286:105–108. [PubMed: 8566146]
6. Hepburn MJ, Little PJ, Gringas J, Khun CM. Differential Effects of Naltrindole on Morphine-Induced Tolerance and Physical Dependence in Rate. J Pharmacol Exp Ther. 1997; 281:1350–1356. [PubMed: 9190871]
7. Purington LC, Sobczyk-Kojiro K, Pogozheva ID, Traynor JR, Mosberg HI. Development and in vitro characterization of a novel bifunctional mu-agonist/delta-antagonist opioid tetrapeptide. ACS Chem Biol. 2011; 6:1375–1381. [PubMed: 21958158]
8. Anand JP, Purington LC, Pogozheva ID, Traynor JR, Mosberg HI. Modulation of Opioid Receptor Ligand Affinity and Efficacy Using Active and Inactive State Receptor Models. Chem Biol Drug Des. 2012; 80:763–770. [PubMed: 22882801]
9. Schiller PW, Fundytus ME, Merovitz L, Weltrowska G, Nguyen TM, Lemieux C, Chung NN, Coderre TJ. The opioid mu agonist/delta antagonist DIPP-NH(2)[Psi] produces a potent analgesic effect, no physical dependence, and less tolerance than morphine in rats. J Med Chem. 1999; 42:3520–3526. [PubMed: 10479285]
10. Balboni G, Guerrini R, Salvadori S, Bianchi C, Rizzi D, Bryant SD, Lazarus LH. Evaluation of the Dmt-Tic pharmacophore: conversion of a potent delta-opioid receptor antagonist into a potent delta agonist and ligands with mixed properties. J Med Chem. 2002; 45:713–720. [PubMed: 11806723]
11. Balboni G, Salvadori S, Trapella C, Knapp BI, Bidlack JM, Lazarus LH, Peng X, Neumeyer JL. Evolution of the Bifunctional Lead mu Agonist/delta Antagonist Containing the Dmt-Tic Opioid Pharmacophore. ACS Chem Neurosci. 2010; 1:155–164. [PubMed: 20352071]
12. Ananthan S, Saini SK, Dersch CM, Xu H, McGlinchey N, Giuvelis D, Bilsky EJ, Rothman RB. 14-Alkoxy- and 14-acyloxypyridomorphinans: μ agonist/δ antagonist opioid analgesics with diminished tolerance and dependence side effects. J Med Chem. 2012; 55:8350–8363. [PubMed: 23016952]
13. Li Y, Lefever MR, Muthu D, Bidlack JM, Bilsky EJ, Polt R. Opioid glycopeptide analgesics derived from endogenous enkephalins and endorphins. Future Med Chem. 2012; 4:205–226. [PubMed: 22300099]
14. El-Andaloussi S, Holm T, Langel U. Cell-Penetrating Peptides: Mechanisms and Applications. Curr Pharmaceut Des. 2005; 11:3597–3611.
15. Egleton RD, Davis TP. Development of Neuropeptide Drugs that Cross the Blood-Brain Barrier. NeuroRx. 2005; 2:44–53. [PubMed: 15717056]
16. Wang C, McFadyen IJ, Traynor JR, Mosberg HI. Design of a high affinity peptidomimetic opioid agonist from peptide pharmacophore models. Bioorg Med Chem Lett. 1998; 8:2685–2688. [PubMed: 9873603]
17. Mathre DJ, Thompson AS, Douglas AW, Hoogsteen K, Carroll JD, Corey EG, Grabowski EJ. ractical process for the preparation of tetrahydro-1-methyl-3, 3-diphenyl-1H, 3H-pyrrolo[1, 2-c][1, 3, 2]oxazaborole-borane. A highly enantioselective stoichiometric and catalytic reducing agent. J Org Chem. 1993; 58:2880–2888.
18. Ohn, V.; Maillard, M.; Tucker, J.; Jagodzinska, B.; Brogley, L.; Tung, J.; Shah, N.; Neitz, JR. Substituted hydroxyethylamine aspartyl protease inhibitors. Patent application WO2005/87752 A2. 2005.
19. Mitsunobu O, Wada M, Sano TJ. Stereospecific and stereoselective reactions. I. Preparation of amines from alcohols. J Am Chem Soc. 1972; 94:679–680.
20. Lee KO, Akil H, Woods JH, Traynor JR. Differential Binding Properties of Oripavines at Cloned Mu- and Delta-Opioid Receptors. Eur J Pharmacol. 1999; 378:323–330. [PubMed: 10493109]

21. Husbands SM, Neilan CL, Broadbear J, Grundt P, Breeden S, Aceto MD, Woods JH, Lewis JW, Traynor JR. BU74, A Complex Oripavine Derivative with Potent Kappa Opioid Receptor Agonism and Delayed Opioid Antagonism. Eur J Pharmacol. 2005; 509:117–135. [PubMed: 15733546]
22. Traynor JR, Nahorski SR. Modulation by Mu-Opioid Agonists of Guanosine-5′-O(3-[35S]thio)triphosphate Binding to Membranes from Human Neuroblastoma SHY5Y Cells. Mol r Pharmacol. 1995; 47:848–854.
23. Lamberts JT, Jutkiewicz EM, Mortensen RM, Traynor JR. Mu-Opioid Receptor Coupling to Gα(o) Plays an Important Role in Opioid Antinociception. Neuropsychopharmacology. 2011; 36:2041–2053. [PubMed: 21654736]
24. Purington LC, Pogozheva ID, Traynor JR, Mosberg HI. Pentapeptides displaying mu opioid receptor agonist and delta opioid receptor partial agonist/antagonist properties. J Med Chem. 2009; 52:7724–7731. [PubMed: 19788201]
25. Hajipour AR, Zarei A, Khazdooz L, Ruoho AE. Simple and Efficient Procedure for the Friedel–Crafts Acylation of Aromatic Compounds with Carboxylic Acids in the Presence of P_2O_5/Al_2O_3 Under Heterogeneous Conditions. Synth Comm. 2009; 39:2702–2722.
26. Bandgar BP, Bettigeri SV, Phopase JJ. Palladium catalyzed ligand-free Suzuki cross-coupling reactions of benzylic halides with aryl boronic acids under mild conditions. Tetrahedron Lett. 2004; 45:6959–6962.
27. Schmidt RG, Bayburt Erol K, Latshaw SP, Koenig JR, Daanen JF, McDonald HA, Bianchi BR, Zhong C, Joshi S, Honore P, Marsh KC, Lee CH, Faltynek CR, Gomtsyan AL. Chroman and tetrahydroquinoline ureas as potent TRPV1 antagonists. Bioorg Med Chem Lett. 2011; 21:1338–1341. [PubMed: 21315587]
28. Volkow ND. Opioid-dopamine interactions: implications for substance use disorders and their treatment. Biol Psych. 2010; 68:685–686.
29. Bowen CA, Negus SS, Zong R, Neumeyer JL, Bidlack JM, Mello NK. Effects of mixed-action kappa/mu opioids on cocaine self-administration and cocaine discrimination by rhesus monkeys. Neuropsychopharmacology. 2003; 28:1125–1139. [PubMed: 12637953]
30. Dietis N, Guerrini R, Calo G, Salvadori S, Rowbotham DJ, Lambert DG. Simultaneous targeting of multiple opioid receptors: a strategy to improve side-effect profile. Br J Anaesth. 2009; 103:38–49. [PubMed: 19474215]
31. Horan PJ, Mattia A, Bilsky EJ, Weber S, Davis TP, Yamamura HI, Malatynska E, Appleyard SM, Slaninova J, Misicka A, Lipkowski AW, Hruby VJ, Porreca F. Antinociceptive profile of biphalin, a dimeric enkephalin analog. J Pharmacol Expt Ther. 1993; 265:1446–1454.
32. Li Y, Lefever MR, Muthu D, Bidlack JM, Bilsky EJ, Polt R. Opioid glycopeptide analgesics derived from endogenous enkephalins and endorphins. Future Med Chem. 2012; 4:205–226. [PubMed: 22300099]
33. Lee YS, Kulkarani V, Cowell SM, Ma S, Davis P, Hanlon KE, Vanderah TW, Lai J, Porreca F, Vardanyan R, Hruby VJ. Development of potent μ and δ opioid agonists with high lipophilicity. J Med Chem. 2011; 54:382–386. [PubMed: 21128594]
34. Lowery JJ, Raymond TJ, Giuvelis D, Bidlack JM, Polt R, Bilsky EJ. In vivo characterization of MMP-2200, a mixed δ/μ opioid agonist, in mice. J Pharmacol Expt Ther. 2011; 336:767–778.
35. Jiang Q, Mosberg HI, Porreca F. Modulation of the potency and efficacy of mu-mediated antinociception by delta agonists in the mouse. J Pharmacol Expt Ther. 1990; 254:683–689.
36. Neilan CL, Husbands SM, Breeden S, Ko MC, Aceto MD, Lewis JW, Woods JH, Traynor JR. Characterization of the complex morphinan derivative BU72 as a high efficacy, long-lasting mu-opioid receptor agonist. Eur J Pharmacol. 2004; 499:107–116. [PubMed: 15363957]

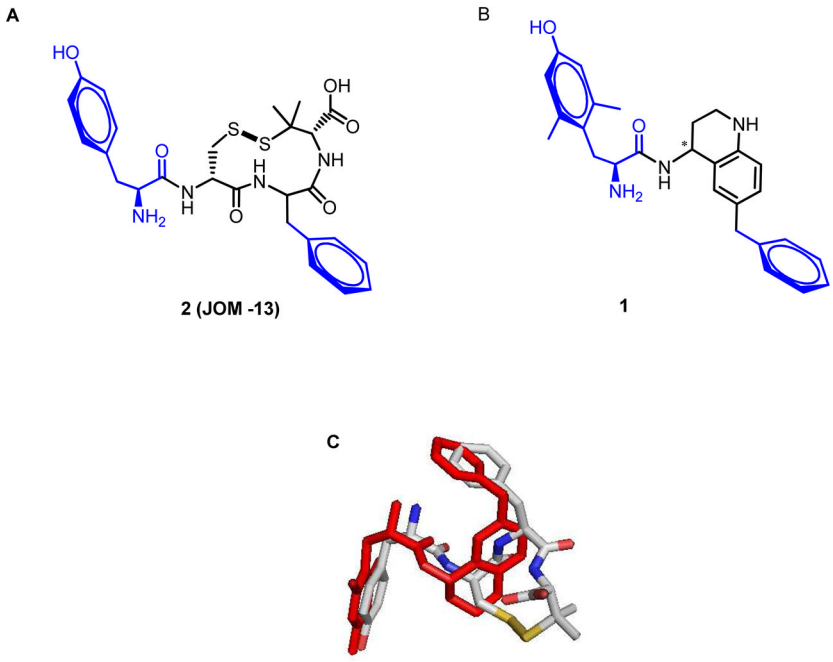

Figure 1.

A. Structure of lead peptide 2 (**JOM-13**, Tyr-c(SS)[DCys-Phe-DPen]OH). B. Structure of lead peptidomimetic **1**(*4R*). C. Superposition of proposed bioactive conformations of **JOM-13** and **1**(*4R*). (see [16]).

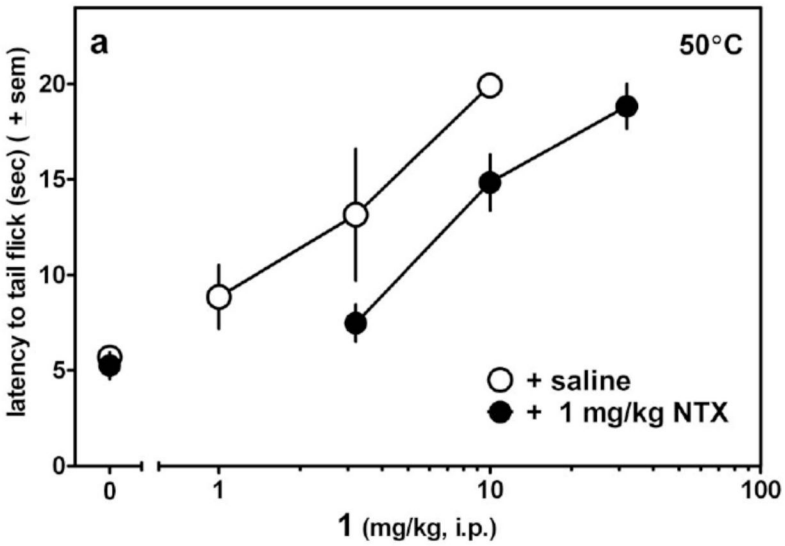

Figure 2.

Antinociceptive activity of **1**(4*R*) in mouse Warm Water Tail Withdrawal (WWTW) assay following intraperitoneal (ip) administration. Data represent response following pretreatment (−30 min) with saline (open circles) or naltrexone (NTX, filled circles) given by *ip* injection.

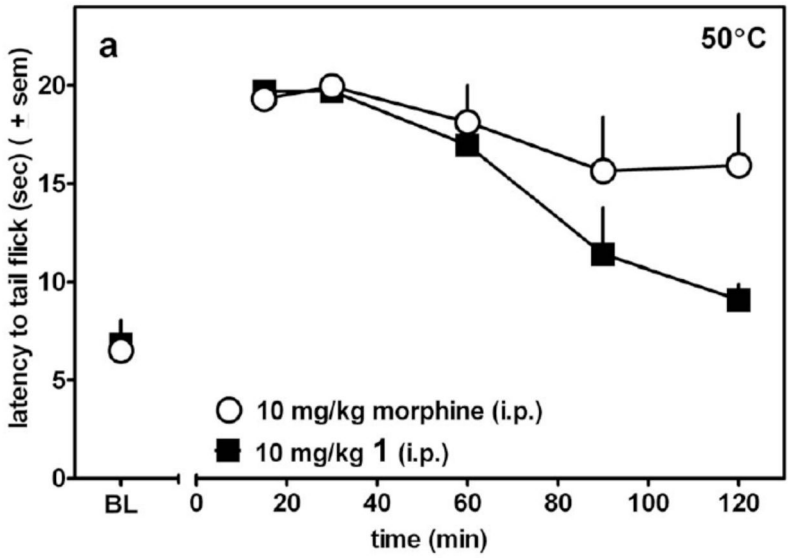

Figure 3.
Time course of antinociception (WWTW assay) of **1**(4*R*) (filled squares) and morphine (open circles) following *ip* administration.

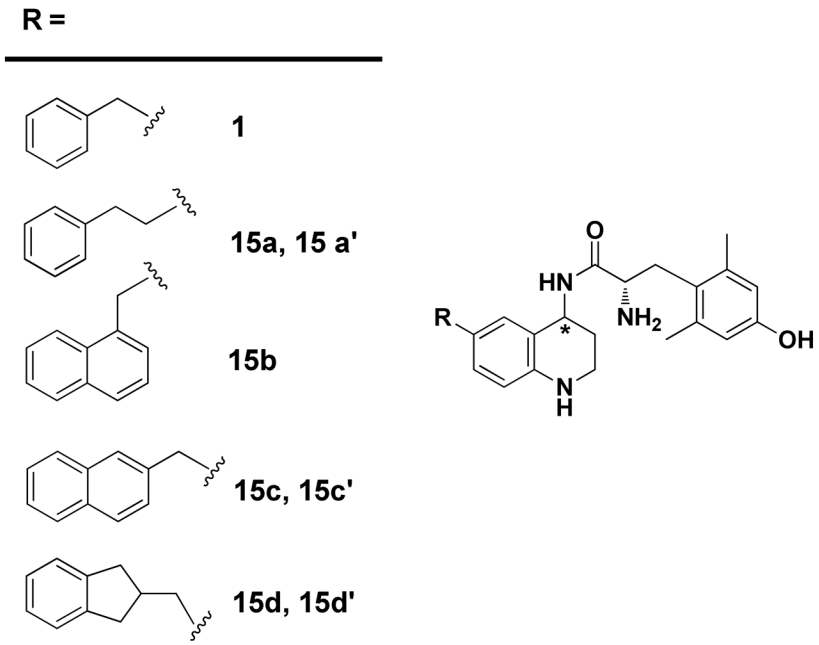

Figure 4.
Structures of Peptidomimetics.

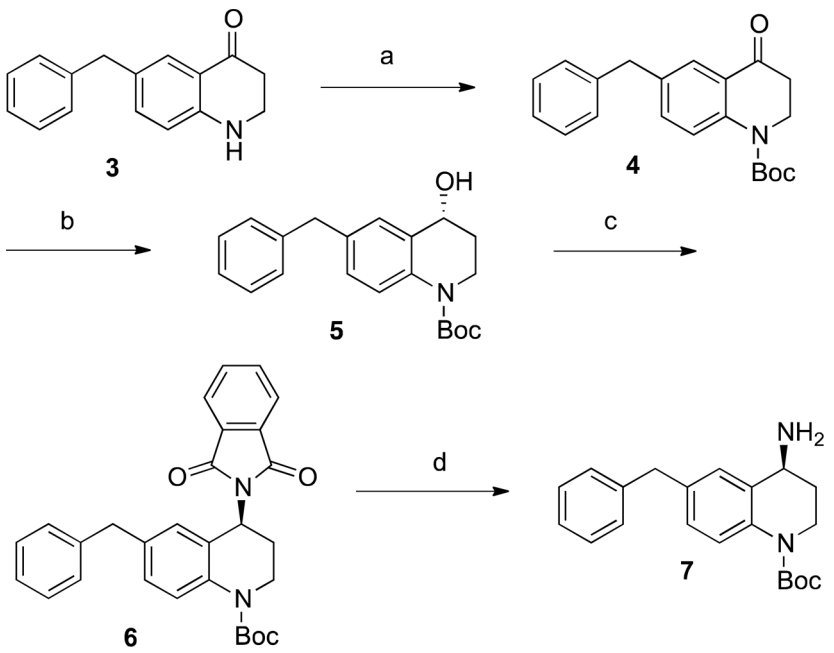

Scheme 1. Asymmetric Synthesis of Compound 7[a]

[a]Reagents and conditions: (a) $(Boc)_2O$, DMAP, DIEA, DCM, reflux; (b) (*S*)-2-methyl-CBS-oxazoborolidine, $BH_3{\cdot}Me_2S$, THF; (c) phthalimide, DIAD, PPh_3, THF; (d) $N_2H_4{\cdot}H_2O$, EtOH.

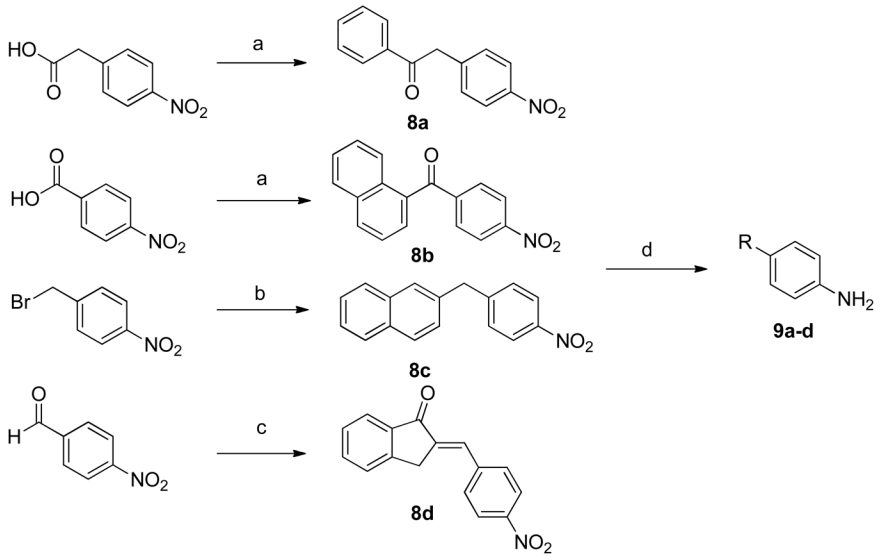

Scheme 2. Preparation of Compounds 9a–d[a]

[a]Reagents and conditions: (a) benzene or naphthalene, P_2O_5, Al_2O_3, reflux; (b) 2-naphthalenyl boronic acid, $PdCl_2$, K_2CO_3, acetone, H_2O, 110°C, microwave irradiation; (c) 1-indanone, KOH, MeOH; (d) 10% Pd/C, H_2, HCl, MeOH.

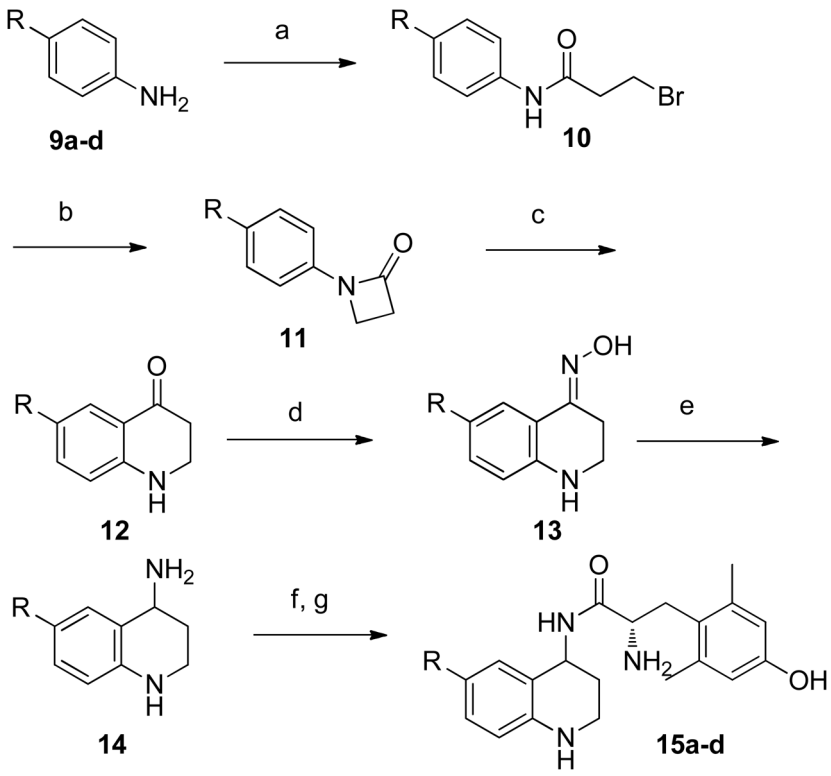

Scheme 3. Preparation of Compounds 15a–d[a]

[a]Reagents and conditions: (a) 3-bromopropionyl chloride, K_2CO_3, DCM; (b) NaO*t*Bu, DMF; (c) TfOH, DCE; (d) $NH_2OH{\cdot}HCl$, NaOAc, EtOH, H_2O, reflux; (e) 10% Pd/C, H_2, AcOH, MeOH; (f) Boc-Dmt, PyBOP, HOBt-Cl, DIEA, DMF; (g) TFA, DCM.

Table 1

Opioid receptor binding affinities of peptidomimetics.

Ki (nM) Binding			
Compound	**MOR**	**DOR**	**KOR**
1 (*4R*) *	0.22 ± 0.02	9.4 ± 0.8	68 ± 2
15a	0.24 ± 0.02	8.9 ± 1.5	25 ± 1
15b	0.76 ± 0.14	6.0 ± 0.7	17 ± 1
15c	0.078 ± 0.007	10 ± 2	54 ± 7
15d	0.16 ± 0.04	4.1 ± 1.6	1.2 ± 0.4
morphine†	6.3 ± 2.5	171 ± 18.9	60.9 ± 17.3
1 (*4S*) *	2.6 ± 0.3	56 ± 5	220 ± 48
15a′	16 ± 2.6	120 ± 15	1200 ± 290
15c′	1.6 ± 0.4	66 ± 1	130 ± 9
15d′	8.0 ± 0.8	180 ± 14	110 ± 9

Binding affinities (K_i) were obtained by competitive displacement of radiolabeled [^{3}H] diprenorphine in membrane preparations. All values are expressed as mean ± SEM of three separate assays performed in duplicate.

*From 16

†From 36

Table 2

Opioid receptor efficacy of peptidomimetics

	EC_{50}(nM)			% Stimulation		
Compound	**MOR**	**DOR**	**KOR**	**MOR**	**DOR**	**KOR**
1 (*4R*)	1.6 ± 0.3	110 ± 6	540 ± 72	81 ± 2	16 ± 2	22 ± 2
15a	1.1 ± 0.3	dns	dns	45 ± 5	dns	dns
15b	0.84 ± 0.35	69 ± 35	dns	93 ± 5	15 ± 1	dns
15c	0.53 ± 0.08	dns	dns	96 ± 3	dns	dns
15d	0.24 ± 0.03	dns	68 ± 15	86 ± 1	dns	38 ± 2
Morphine *	194 ± 21	nt	nt	57 ± 5		

Efficacy data were obtained using agonist induced stimulation of [^{35}S] GTPγS binding assay. Efficacy is represented as EC_{50} (nM) and percent maximal stimulation relative to standard agonists DAMGO (MOR), DPDPE (DOR) or U69,593 (KOR) at 10μM concentrations. All values are expressed as mean ± SEM of three separate assays performed in duplicate.

dns: does not stimulate; nt: not tested.

*From 7.